1. Supporting Information

Nitrogen-doped carbon dots alleviate the damage from tomato bacterial wilt syndrome: systemic acquired resistance activation and reactive oxygen species scavenging

Xing Luo[a], Xuesong Cao[a], Chuanxi Wang[a], Le Yue[a], Xiaofei Chen[a], Hanyue Yang[a], Xiehui Le[a], Xiaoli Zhao[b], Fengchang Wu[b], Zhenyu Wang[a,*], Baoshan Xing[c]

[a]*Institute of Environmental Processes and Pollution control, and School of Environment and Civil Engineering, Jiangnan University, Wuxi 214122, China*

[b]*State Key Laboratory of Environmental Criteria and Risk Assessment, Chinese Research Academy of Environmental Sciences, Beijing, 100012, China*

[c]*Stockbridge School of Agriculture, University of Massachusetts, Amherst, Massachusetts 01003, United States*

*Corresponding author:

Tel.:+86 0510 85911123; Fax:+86 0510 85911123

E-mail address: wang0628@jiangnan.edu.cn (Dr. Zhenyu Wang)

Number of pages: 13
Number of figures: 9
Number of tables: 5

Experiment S1: Oxidative stress and antioxidative enzyme activity analysis

The oxidative stress of tomato leaves was characterized by the ROS level. The accumulation of ROS in tomato leaves was determined using the fluorescent probe 2′,7′-dichlorodihydrofluorescein diacetate (H2DCFDA).[1] Briefly, fresh leaf discs (diameter: 5 mm) were incubated in H2DCFDA (25 μM) for 30 min in dark, with subsequent washing three times in PBS (pH=7.0). The dyed leaf discs were imaged using a confocal laser scanning microscopy (CLSM, Nikon A1, Japan) with an excitation wavelength at 488 nm, and the relative ROS levels were analyzed according to the green fluorescence intensity in tomato leaves with the software of Image J.

The antioxidant efficacy of carbon-based nanomaterial was conducted by *in vitro* 2-2-diphenyl-1-di-picryl-hydrazyl (DPPH) free radical assay with some modification.[3] Briefly, 200 μL reaction mixture (100 mg/L DPPH and the treatments of N-CDs, PAA-N-CDs, P-CDs, and butylated hydroxytoluene (BHT, as the positive control) at 10, 50,100, and 250 mg/L in absolute ethanol) was incubated in dark for 30 min and then measured by a spectrophotometer (Ratastie 2, FI-01620 Vantaa, Finland) at 517 nm.

The hydrogen peroxide (H_2O_2) *in vivo* detection was performed according to Ma *et al.*[4] Briefly, tomato leaves were infiltrated by 3,3'-diaminobenzidine solution (1 g/L, pH 3.8, 5 h) under the vacuum condition. Tomato leaves were heated in 95% ethanol to remove the chlorophylls. Then, the samples were pictured and the relative H_2O_2 level was analyzed using the software of Image J.

The activity of CAT, POD, and SOD, was determined according to a previous study with slight modifications.[5] Briefly, tomato leaves (200 mg) were ground in 50 mM pre-cooled PBS (pH7.8) containing 1% polyvinylpyrrolidone. The homogeneous was centrifuged (12000 g, 4 °C, 20 min), and the supernatants were enzyme extracts. SOD activity was determined by photochemical NBT method in 3 mL reaction mixture. The reaction mixture, including 50 mM PBS (pH 7.8), 75 μM NBT, 10 μM EDTA-Na_2, 13.05 mM methionine, 2 μM riboflavin, and 100 μL enzyme extracts, was shaken and exposed to light for 20 min. Two hundred μL of the reaction mixture was transferred to a multifunctional microplate and measured at 560 nm using a spectrophotometer. One unit of SOD is defined as being present in the extract, which can inhibit by 50% of NBT photoreduction. POD activity was measured with guaiacol as the substrate. The absorbance of 200 μL reaction mixture (20 mM potassium phosphate buffer (pH 6.0), 0.56% guaiacol, 0.01% H_2O_2, and 6.67 μL enzyme extracts) was recorded for 3 min at 470 nm. The increase of 0.01 of OD value per min was defined as one unit of POD. For CAT activity, the absorbance of 200 μL of the reaction mixture (15 mM phosphate buffer (pH 7.0), 0.05% H_2O_2, and 6.67 μL enzyme extracts) was recorded for 3 min at 240 nm. The reduction of 0.01 of OD value per min was used as one unit of CAT.

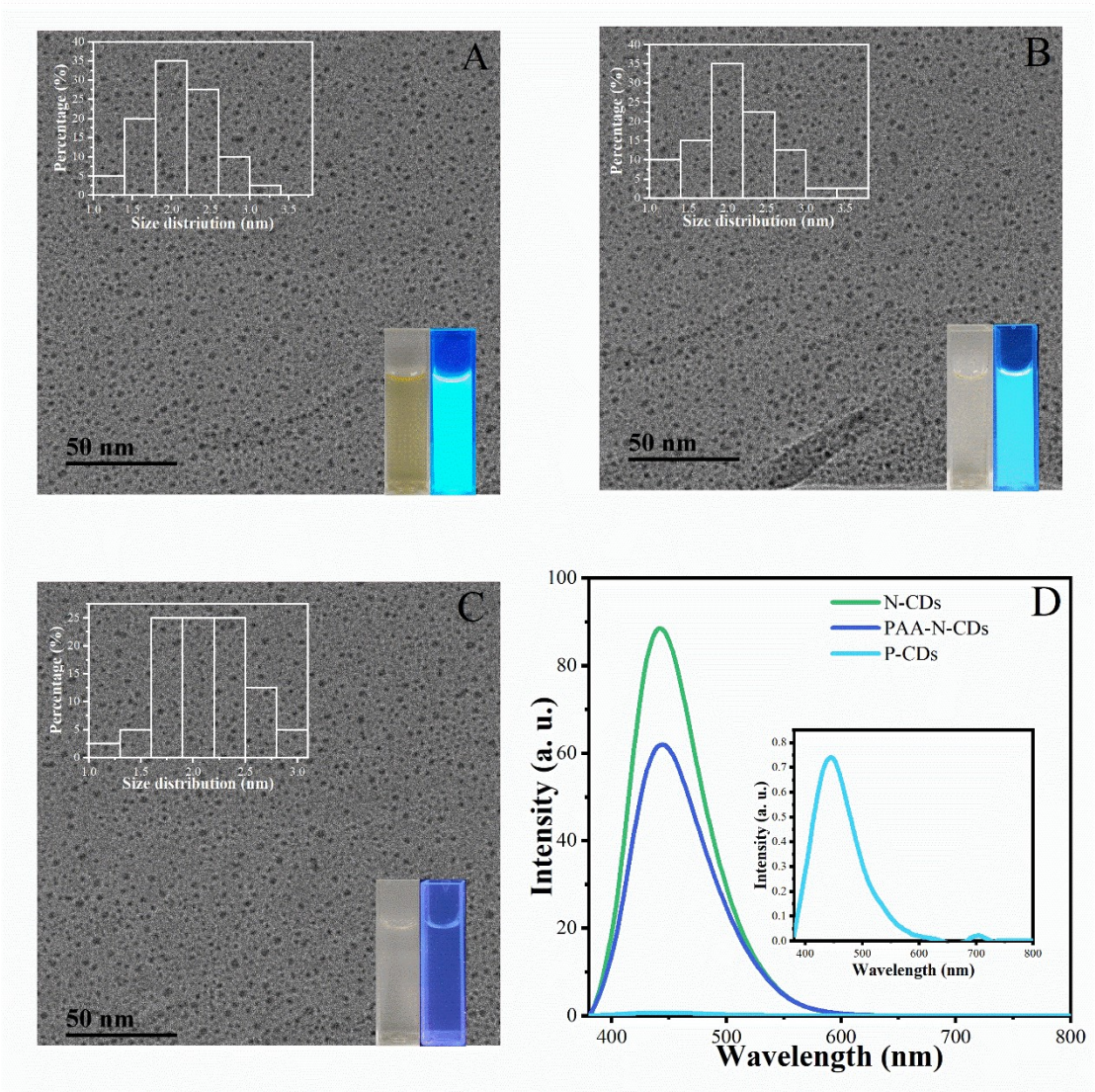

Figure S1. TEM images of nitrogen doped CDs (N-CDs), polyacrylic acid (PAA) coated N-CDs (PAA-N-CDs), and pure CDs (P-CDs) (upper left inset: normal distribution of the size of three CDs; lower right inset: the photographs of three CDs under the irradiation of 365 nm light); (D) The fluorescence spectra of N-CDs, PAA-N-CDs, and P-CDs NMs at 360 nm light irradiation (inset: the magnification of P-CDs spectrum at the range of 380-800 nm).

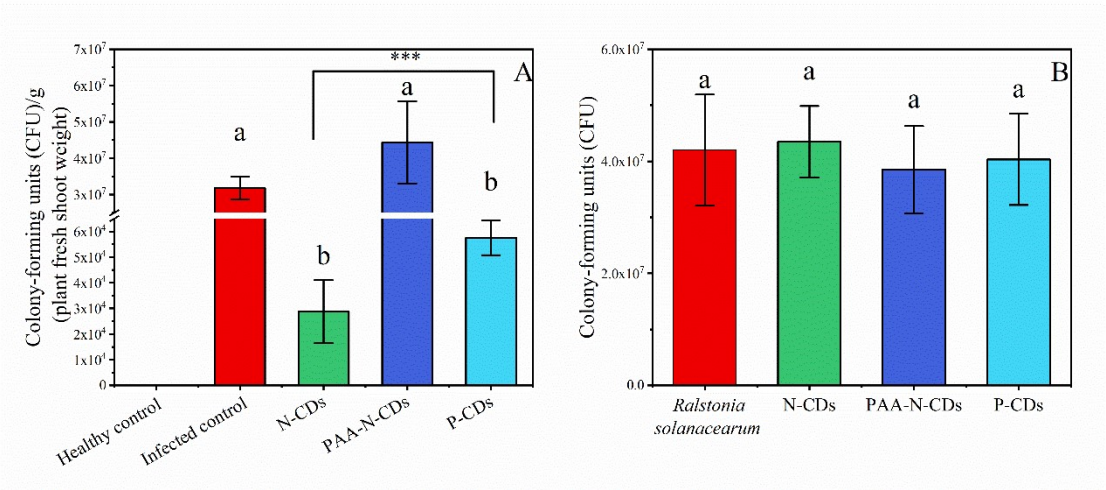

Figure S2. The abundance of *Ralstonia solanacearum* in tomato stems upon foliar application with 10 mg/L N-CDs, PAAN-CDs, and P-CDs, respectively (A). Effect of N-CDs, PAA-N-CDs, and P-CDs at 10 mg/L on the growth of *Ralstonia solanacearum* after 2 days exposure (B). Healthy control represented the tomatoes were not infected by *Ralstonia solanacearum* and not foliarly applied with CDs. Infected control represented the tomatoes were infected by pathogens and not foliarly applied with CDs. The significant difference among different treatments is marked with different letters ($p < 0.05$, Duncan, n = 6). The significant difference of the treatment of N-CDs and P-CDs is marked with *** ($p < 0.001$, *t* test, n=6).

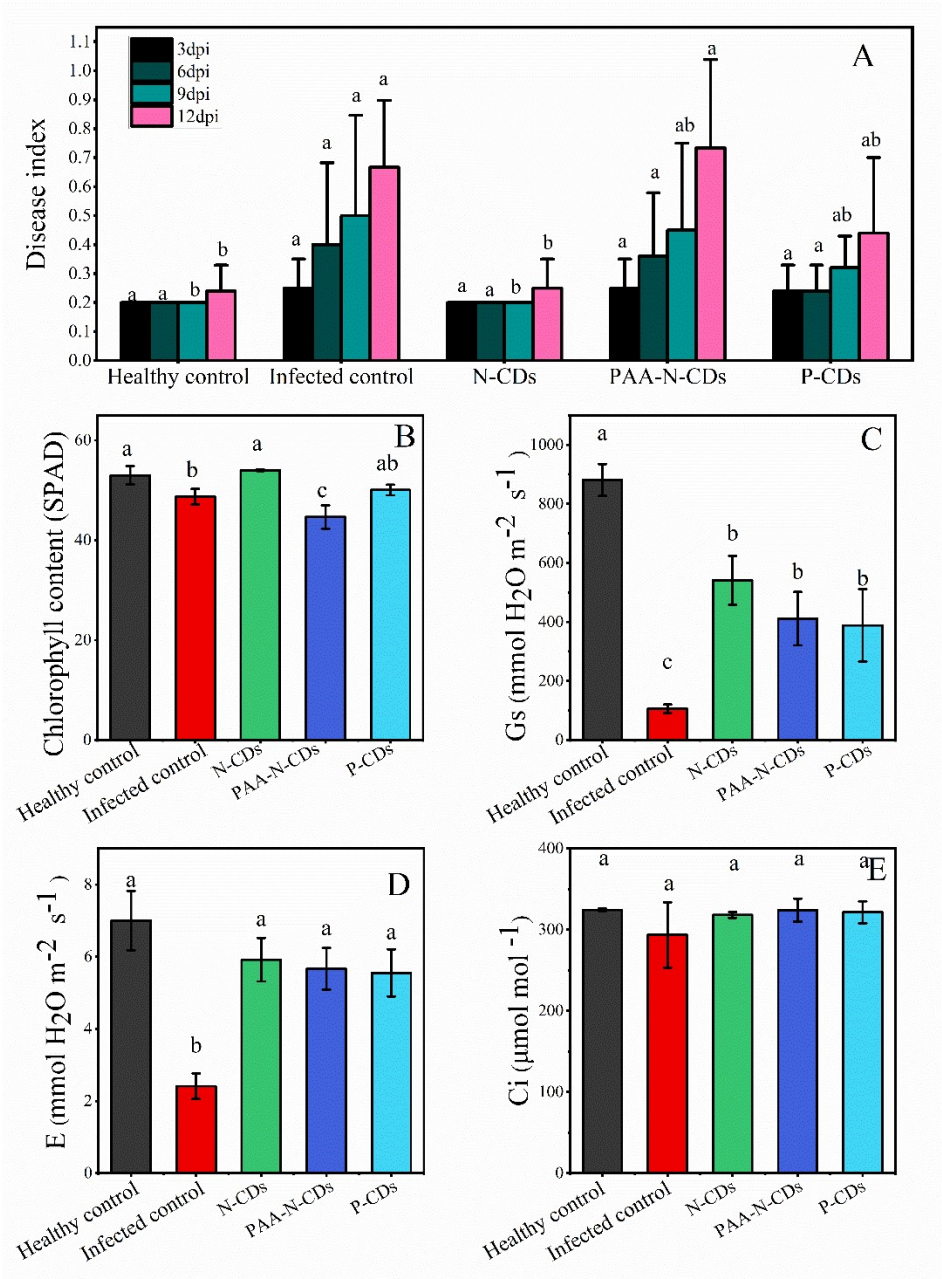

Figure S3. Disease incidence of *Ralstonia solanacearum*-infected tomatoes from first time of foliar application to harvest after foliar application with 10 mg/L N-CDs, PAAN-CDs, and P-CDs (A). Chlorophyll content (single photon avalanche diode, SPAD) (B), stomatal conductance (Gs) (C), transpiration rate (E) (D), and intracellular CO_2 concentrations (Ci) (E) of *Ralstonia solanacearum*-infected tomatoes upon foliar application with 10 mg/L N-CDs, PAA-N-CDs, and P-CDs, respectively. Healthy control represented the tomatoes were not infected by *Ralstonia solanacearum* and not foliarly applied with CDs. Infected control represented the tomatoes were infected by pathogens and not foliarly applied with CDs. The significant difference among different treatments is marked with different letters ($p < 0.05$, Duncan, n = 6).

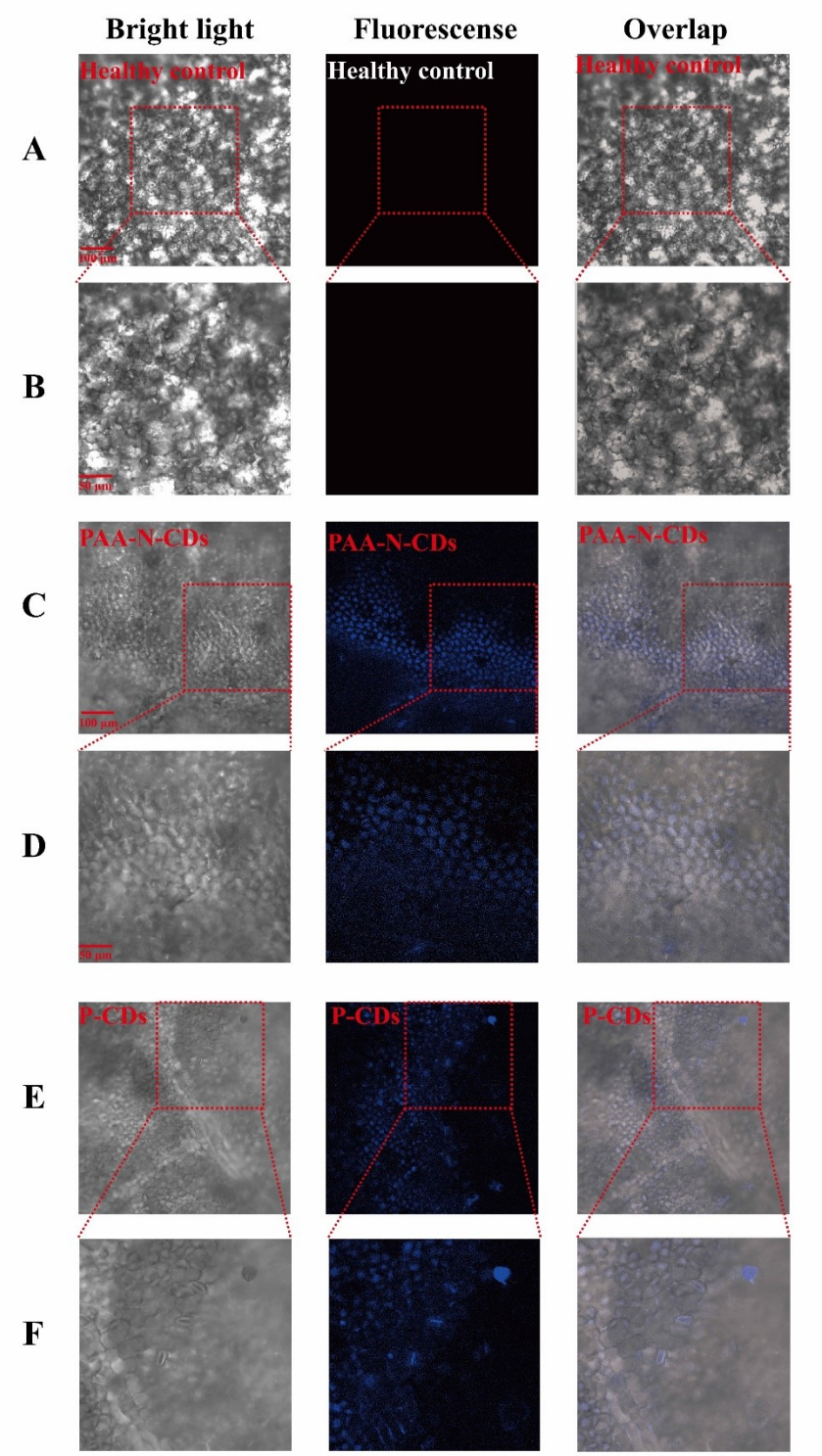

Figure S4 Confocal laser scanning microscopy images of tomato leaves in healthy control (A and B), 10 mg/L PAA-N-CDs treatment (C and D), and 10 mg/L P-CDs treatment (E and F). Panel B, D and F were enlarged from the red squares of panel A, C and E. The excitation wavelength is 405 nm.

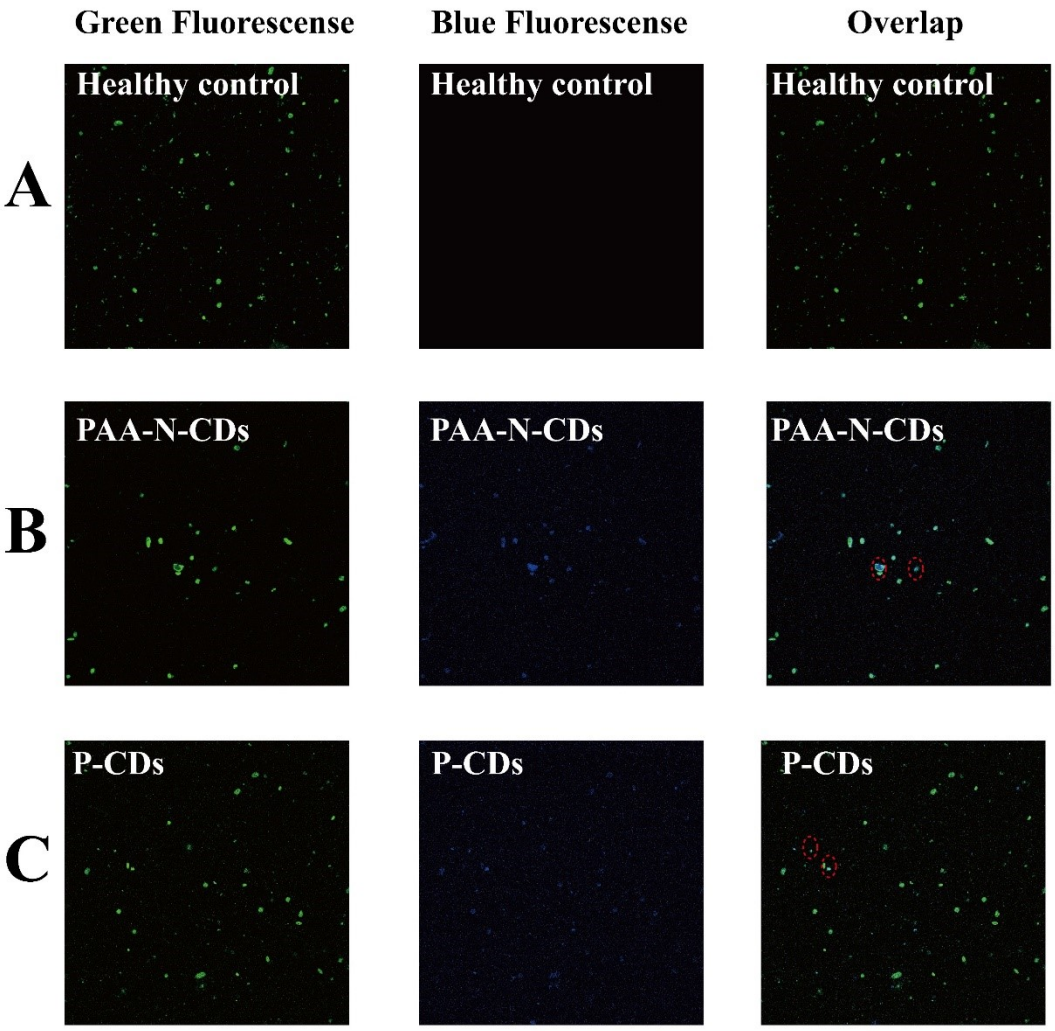

Figure S5. Confocal images of chloroplasts extracted from the tomato leaves in healthy control (A), 10 mg/L PAA-N-CDs treatment (B), and P-CDs treatment (C). The excitation wavelength for chloroplasts and N-CDs is 488 and 405 nm. The green fluorescence indicated that the presence of chloroplasts. The blue fluorescence demonstrated that the presence of PAA-N-CDs and P-CDs.

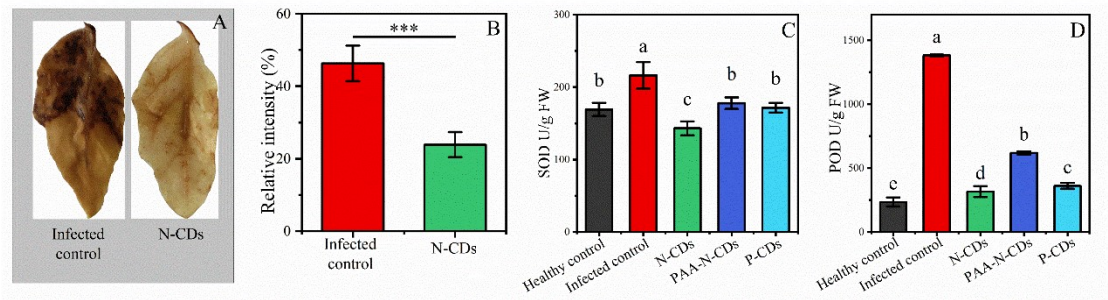

Figure S6. H_2O_2 production in pathogen infected tomato leaves upon foliar application of N-CDs at 0 and 10 mg/L as indicated by the photograph (A) and relative intensity (B). The significant difference between infected control and the treatment of N-CDs is marked with "***" (p < 0.001, t test, n=6); superoxide dismutase (SOD) (C) and peroxidase (POD) (D) activity in tomato leaves from healthy control, infected control, N-CDs treatment, PAA-N-CDs treatment, and P-CDs treatment. The significant difference among different treatments is marked with different letters (p< 0.05, Duncan, n = 6).

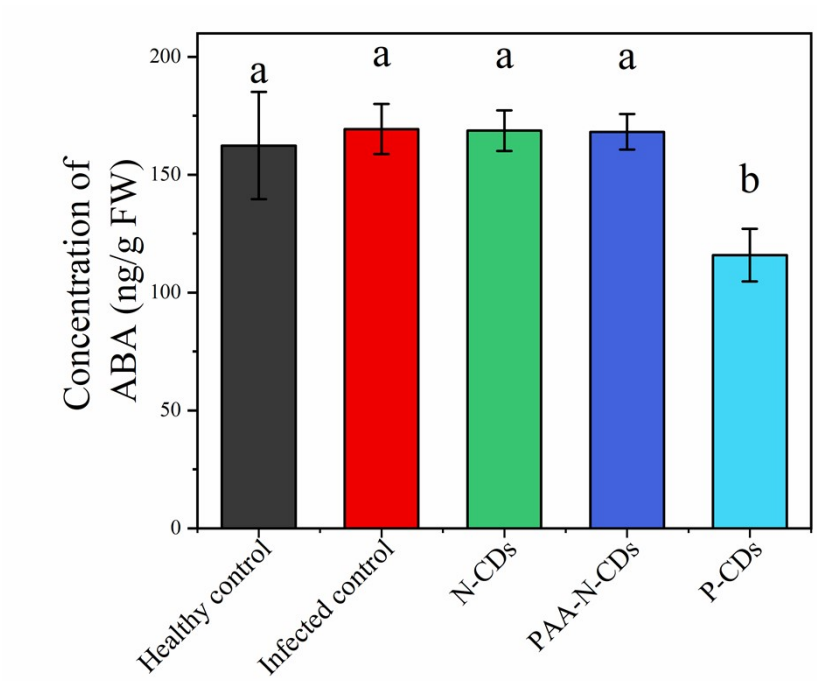

Figure S7. Abscisic acid (ABA) content in tomato shoots from healthy control, infected control, N-CDs treatment, PAA-N-CDs treatment, and P-CDs treatment. The significant difference among different treatments is marked with different letters (p< 0.05, Duncan, n = 6).

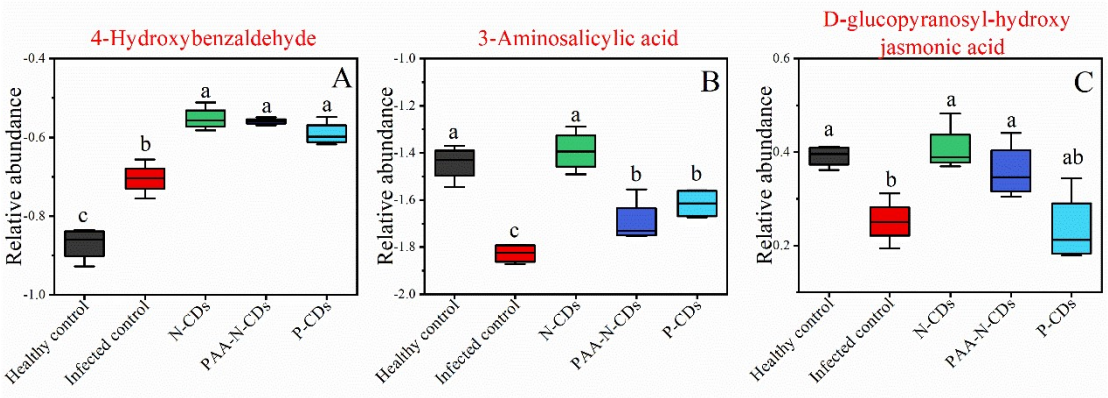

Figure S8. Box-whisker plots of relative abundance of SA (A-B) and JA (C) biosynthesis of metabolites in tomato leaves from healthy control, infected control, N-CDs treatment, PAA-N-CDs treatment, and P-CDs treatment. The significant difference among different treatments is marked with different letters ($p < 0.05$, Duncan, n = 4).

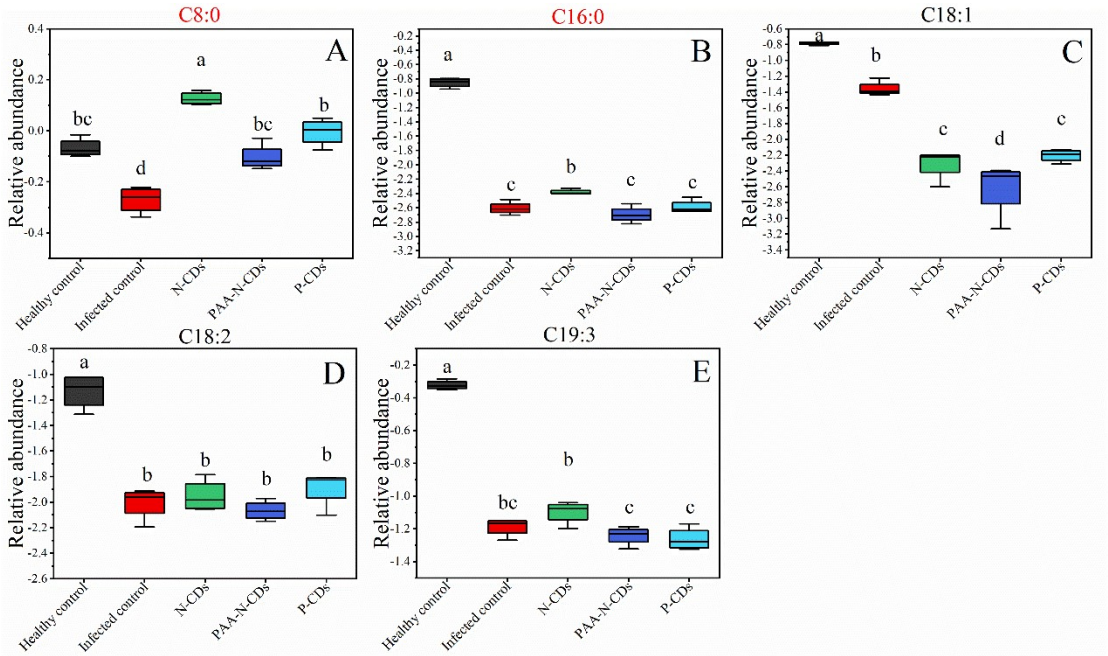

Figure S9. Box-whisker plots of relative abundance of fatty acid in tomato leaves from healthy control, infected control, N-CDs treatment, PAA-N-CDs treatment, and P-CDs treatment. The significant difference among different treatments is marked with different letters ($p < 0.05$, Duncan, n = 4).

Table S1 Primers used in qRT-PCR.

Gene name	Gene ID	Forward prime (5′-3′)	Reverse primer (5′-3′)
Actin	NM_001321306	TGTCCCTATCTACGAGGGTTATGC	CAGTTAAATCACGACCAGCAAGA
P4	NM_001247594	GCAACAATGGGTGGTGGTTC	ACCTAAGCCACGATACCATGA
PTI5	NM_001247058	GCGATTCGGCTAGACATGGT	CCTCGCATTCTAAAAGCCGC
PR5	NM_001330783	GGCCCATGTGGTCCTACAAA	GGCAACATAGTTTAGCAGACCG
PR1A2	NM_001321040	GTAGGCAATTGGGTCGGACA	ACTTAAGCCCACTATACCATGAAC A
PR1	XM_004242627	TGCAAAATGGTGGGCAAATTCA	GCCCAAGCATTAACGGCATC
JA2	NM_001247043	ACGGGGACGGATAAGGTGAT	GCACCCATTCATCTAGCTTTGAA
MPK1	NM_001247082	TCCCAGAAGGAGAATAACAGTTG A	CTGCAACAATCTGTCAGCAAT
PAL	NM_001320040	CACTGTAAGCCAAGTAGCCAAAA	GAGCTGCAGGGGTCATCAG

Note: The RT-PCR primers were designed and followed by Ye et al.[6] based on the genome of Solanum lycopersicum (tomato, ID: 4081) in National Center for Biotechnology Information Search database (https://www.ncbi.nlm.nih.gov/). The accuracy of designed primers was verified by performing against the NCBI RefSeq mRNA database with organism limited to Solanum lycopersicum.

Table S2 Characterization of N-CDs, PAA-N-CDs, P-CDs.

	Diameter (nm)	Hydraulic diameter (nm)	Zeta potential (mV)
N-CDs	2.08±0.46a	244.04±38.95b	-10.53±1.32b
PAA-N-CDs	2.13±0.51a	169.63±12.14c	-15.45±2.09c
P-CDs	2.10±0.40a	334.43±25.95a	14.90±2.95a

Table S3 Weight of pathogen infected tomato shoots and roots after foliar application with 10 mg/L N-CDs, PAA-N-CDs, and P-CDs.

	Treatments	Root	Shoot	Total
Fresh weight（g）	Healthy control	1.26±0.38 a	13.73±1.70 a	14.99±1.91 a
	Infected control	1.36±0.23 a	7.93±0.95 bc	9.29±0.73 b
	N-CDs	1.58±0.24 a	12.36±0.77 a	13.94±1.01 a
	PAA-N-CDs	1.13±0.11 a	6.37±1.75 c	7.50±1.86 b
	P-CDs	1.84±0.65 a	10.82±1.53 ab	12.66±0.88 a
Dry weight (mg)	Healthy control	157.99±39.47ab	994.85±0.92ab	1152.84±38.55a
	Infected control	115.19±12.14b	748.00±84.80b	863.20±77.78b
	N-CDs	199.88±42.49a	1097.42±220.32a	1297.30±262.81ab

PAA-N-CDs	125.94±37.79ab	822.6±18.37b	948.54±19.41ab
P-CDs	160.07±30.11ab	996.91±76.04ab	1156.99±45.93ab

Table S4 Concentrations of macronutrients (mg/kg) in pathogen infected tomato shoots and roots after foliar application with 10 mg/L N-CDs, PAA-N-CDs, and P-CDs.

	Treatments	S	K	Mg	P	Ca
Shoot	Healthy control	1023.99±157.11b	21144.24±2376.65c	4540.69±709.98b	584.97±70.17b	28350.10±8930.13a
	Infected control	1507.21±184.13a	23695.89±402.14c	6384.64±99.39a	1494.67±309.43a	30135.10±1735.46a
	N-CDs	1053.52±275.31b	37648.23±3489.94a	4372.26±1164.14b	723.60±233.75b	33938.00±2055.38a
	PAA-N-CDs	1366.61±346.35ab	24006.08±3236.55c	7204.00±745.48a	1288.69±487.05a	28516.50±4872.69a
	P-CDs	1331.43±467.70ab	32524.73±4341.15b	4889.15±443.60b	973.10±321.66ab	31434.40±4112.35a
Root	Healthy control	1591.21±565.47b	17834.13±2610.55a	8130.21±1107.42a	1254.26±126.05bc	17724.67±1089.37a
	Infected control	2197.59±115.80a	18350.39±5570.86a	7788.72±1529.26a	1556.26±192.91a	20220.00±2149.85a
	N-CDs	1567.13±166.18b	15338.23±3622.32a	5617.21±1344.15b	1016.68±127.38c	19901.50±3205.48a
	PAA-N-CDs	2041.95±167.96a	15805.22±3901.17a	6647.39±918.05ab	1474.32±189.67ab	19810.10±4584.48a
	P-CDs	1917.90±453.48ab	13697.60±4864.95a	7100.41±1353.98ab	1309.29±476.23ab	18186.89±1666.44a

Table S5 Concentrations of micronutrients (mg/kg) in pathogen infected tomato shoots and roots after foliar application with 10 mg/L N-CDs, PAA-N-CDs, and P-CDs.

	Treatments	Zn	Mn	Cu	Fe	Mo
Shoot	Healthy control	89.90±7.98a	25.93±2.98c	6.81±0.42b	2.70±0.03b	2.51±0.16ab
	Infected control	89.38±16.88a	34.80±7.84bc	6.65±0.13b	2.75±0.23b	2.99±0.25a
	N-CDs	98.41±16.82a	49.88±7.69a	8.67±1.01a	11.50±3.92a	2.33±0.26ab
	PAA-N-CDs	88.96±11.57a	40.12±4.75ab	7.99±0.78a	1.14±0.13b	2.35±0.69ab
	P-CDs	76.06±23.93a	30.45±3.96bc	6.46±0.48b	1.13±0.28b	2.06±0.12b
Root	Healthy control	49.90±17.57a	95.46±19.47a	36.67±4.30a	59.05±13.19a	1.38±0.13b
	Infected control	47.13±3.01a	99.42±42.02a	33.45±2.61a	44.05±26.16a	1.58±0.20a
	N-CDs	53.83±5.54a	84.14±10.79a	35.68±8.39a	47.41±13.97a	1.59±0.05a
	PAA-N-CDs	44.57±3.59a	106.11±13.61a	30.43±7.04a	40.12±4.13a	1.52±0.12ab
	P-CDs	47.40±11.97a	88.25±11.20a	30.78±5.45a	41.52±8.88a	1.39±0.04b

References

1. Y. L. Liu, L. Yue, C. X. Wang, X. S. Zhu, Z. Y. Wang and B. S. Xing, Photosynthetic response mechanisms in typical C3 and C4 plants upon La_2O_3 nanoparticle exposure, *Environ. Sci.: Nano*, 2020, **7**, 81-92.
2. H. Wu, N. Tito and J. P. Giraldo, Anionic cerium oxide nanoparticles protect plant photosynthesis from abiotic stress by scavenging reactive oxygen species, *ACS Nano*, 2017, **11**, 11283–11297.
3. B. Das, P. Dadhich, P. Pal, P. K. Srivas, K. Bankoti and S. Dhara, Carbon nanodots from date molasses: new nanolights for the *in vitro* scavenging of reactive oxygen species, *J. Mater. Chem. B*, 2014, **2**, 6839-6847.
4. C. X. Ma, H. Liu, H. Y. Guo, C. Musante, S. H. Coskun, B. C. Nelson, J. C. White, B. S. Xing and O. P. Dhankher, Defense mechanisms and nutrient displacement in *Arabidopsis thaliana* upon exposure to CeO_2 and In_2O_3 nanoparticles, *Environ. Sci.: Nano*, 2016, **3**, 1369-

1379.
5. N. Ma, C. Hu, L. Wan, Q. Hu, J. Xiong and C. Zhang, Strigolactones improve plant growth, photosynthesis, and alleviate oxidative stress under salinity in rapeseed (*Brassica napus* L.) by regulating gene expression, *Front. Plant Sci.*, 2017, **8**, 1671.
6. J. Ye, G. Coulouris, I. Zaretskaya, I. Cutcutache, S. Rozen and T. L. Madden, Primer-blast: a tool to design target-specific primers for polymerase chain reaction, *BMC Bioinf.*, 2012, **13**(1), 134.